

Frequency stability of grid-forming power-limiting droop control

Amirhossein Iraniparast and Dominic Groß

Abstract—In this paper, we analyze power-limiting grid-forming droop control used for grid-connected power converters. Compared to conventional grid-forming droop control, power-limiting droop control explicitly accounts for active power limits of the generation (e.g., renewables) interfaced by the converter. While power-limiting droop control has been demonstrated to work well in simulation and experiment, analytical results are not readily available. To address this gap, we first reformulate the dynamics of a power system comprised of converters using power-limiting droop controller as a projected dynamical system in nodal coordinates. Next, we change coordinates from nodal coordinates to edge coordinates to interpret the resulting dynamics as primal-dual dynamics associated with a constrained power flow problem. Leveraging convergence results for primal-dual dynamics, we show that, under mild feasibility assumptions, the frequency dynamics of a power system comprised of converters using power-limiting droop control are globally asymptotically stable with respect to the set of optimizers of its associated constrained power flow problem. Moreover, we show that (i) the converter frequencies synchronize to a common synchronous frequency for each grid-forming converter, and (ii) characterize the synchronous frequency in the case of converters operating at their power limit. Specifically, this result establishes that power-limiting droop control exhibits properties similar to so-called power-sharing in conventional unconstrained droop control.

Index Terms—Grid-forming control, frequency synchronization, power limiting

I. INTRODUCTION

The transition from bulk power generation towards decarbonization and renewable energy sources results in significantly different power system dynamics. In particular, renewable generation is interfaced through power electronic devices that significantly differ from conventional synchronous generators in terms of their response time, device constraints (e.g., power and current limits), and dynamic interactions through the grid. As a result, introducing renewable generation into large-scale power system challenges standard operating and control paradigms and jeopardizes system stability and reliability [1], [2]. Moreover, the constraints of power converters and renewable generation sources such as limited overcurrent, limited overload capability, dc voltage limits, and limited inherent energy storage need to be considered in the stability analysis of emerging power systems.

Today, most renewables are interfaced by dc/ac voltage source converters using so-called grid-following control that

require a stable and slowly changing ac voltage (i.e., magnitude and frequency) irrespective of the power injection by renewables and jeopardizes grid stability when disturbances occur [3]. However, because grid-following control explicitly controls the converter current and dc voltage, incorporating the aforementioned converter constraints and generation limits is straightforward. In contrast, grid-forming converters impose stable and self-synchronizing ac voltage dynamics at their grid terminals and are commonly envisioned to replace synchronous machines as the cornerstone of future power systems. However, loosely speaking, standard grid-forming controls require a fully controllable power source and may destabilize the system due to converter and generation constraints [4].

Prevalent grid-forming controls include droop control [5], virtual synchronous machine control (VSM) [6], and dispatchable virtual oscillator control (dVOC) [7]. Specifically, grid-forming controls mimic the resilient grid-support functions of synchronous machines. However, device constraints remain a significant concern and existing stability results for droop control [8], VSM control [9] and dVOC [10] do not account for power converter or renewable generation constraints. While the majority of theoretical works on grid-forming controls neglects converter constraints, current limiting in grid-forming controls has received significant attention in the application oriented literature [11]–[14] and only a few works investigate dc voltage limits [15] and power limits [16].

The focus of this work is grid-forming control subject to power limits that arise from limits of renewable generation. Notably, this problem is distinct from current limiting, which aims to protect the converter’s semiconductor switches from overcurrent. While power-limiting droop control has been demonstrated to work well in practice, e.g., in the CERTS microgrid testbed [16], to the best of the authors’ knowledge, no analytical stability conditions or theoretical results are available in the literature. To address this gap in the literature, this work reinterprets power-limiting droop control [16] as primal-dual dynamics associated with a constrained power flow problem.

Continuous-time primal-dual gradient descent dynamics are widely used in control and optimization to determine saddle points of the (augmented) Lagrangian associated with constrained convex optimization problems [17]. In the context of power system dynamics, primal-dual dynamics have been used to reverse-engineer and analyze existing system-level control algorithms such as automatic generation control in multi-machine power systems [18] and design distributed power flow control [19]. These works focus on equality constrained optimization problems that arise from secondary and tertiary control of power systems. Instead, in this work we focus on analysis of grid-forming (i.e., primary) control subject

This work was supported in part by the National Science Foundation under Grant No. 2143188. A. Iraniparast and D. Groß are with the Department of Electrical and Computer Engineering at the University of Wisconsin-Madison, USA; e-mail: iraniparast@wisc.edu, dominic.gross@wisc.edu

to inequality constraints modeling generation and converter power limits. To this end, we leverage results that reformulate primal-dual dynamics as a projected dynamical system and establish that their Carathéodory solutions are globally asymptotically stable with respect to the optimal solution of an underlying optimization problem. Specifically, results for strongly convex and continuously differentiable objective function subject to inequality constraints have been obtained using LaSalle functions [17] and a projection free variant of primal-dual dynamics has been introduced to establish global exponential stability and convergence rates [20].

In this work, we provide a deeper insight into the power limit constraints of converters, and investigate the behavior of power-limiting droop control under constraints. Conventional grid-forming droop control is a linear controller that can be understood and analyzed as a Laplacian flow [8]. power-limiting droop control combines conventional droop control with proportional-integral controls that activate when the converter reaches its power limit [16]. First, we reformulate the frequency dynamics of a (Kron-reduced) power system containing converters using grid-forming power-limiting droop control as a projected dynamical system. Notably, the dynamics of grid-forming controls are typically analyzed using so-called nodal coordinates. In contrast, we leverage a change of coordinates to establish that power-limiting droop control is equal to the primal-dual dynamics associated with a constrained power flow problem in so-called edge coordinates [21].

Using these preliminary results and applying them to primal-dual gradient flows of inequality constrained optimization problems [17], we show that a power system containing converters using grid-forming power-limiting droop control is asymptotically stable with respect to Karush-Kuhn-Tucker (KKT) points of the aforementioned constrained power flow problem. Moreover, we establish that the grid-forming converters synchronize to a common synchronous frequency and characterize the synchronous frequency as a function of the overall load in the system relative to the combined power limits of all converters, converter power setpoints, and converter droop coefficients. This result provides deep insights into how power limits impact the synchronous frequency and when converter power limits are active.

In particular, we formally characterize the relationship between the overall load and the active constraint set and synchronous frequency upon convergence of the power system to a KKT point of the constrained power flow problem. Moreover, we establish that, upon convergence, the converters exhibit properties similar to so-called power-sharing [22] in conventional unconstrained droop control. Specifically, power-limiting droop control results in power-sharing up to the power limit, i.e., converters share the additional load according to their droop coefficient until reaching their power limit. This result also establishes that (i) power-limiting droop control cannot converge to operating points at which some converters are at their upper power limit while other converters are at their lower power limit, and that (ii) the synchronous frequency is a function of the overall load, droop coefficients of converters that are not at their power limit, and power limits of converters

that are operating at their power limit. Overall, these results are important from a practical point of view to establish that power-limiting droop control does not converge to counter-intuitive operating points that are not aligned with assumptions of higher-level power system controls and operation.

This paper is organized as follows. Section II introduces the network model, power converter model, and power-limiting droop control. Moreover, we show that the dynamics of a power system with converters using power-limiting droop control can be expressed as a projected dynamical system. Next, Section III defines a constrained dc power flow problem and summarizes our main result, i.e., a network of converters using power-limiting droop control is globally asymptotically stable with respect to an optimal solution of the constrained dc power flow problem. Preliminary results and detailed proofs of the main results are presented in Section IV. Finally, Section V provides conclusions and topics for future work.

Notation

We use \mathbb{R} and \mathbb{N} to denote the set of real and natural numbers and define, e.g., $\mathbb{R}_{\geq 0} := \{x \in \mathbb{R} | x \geq 0\}$. Moreover, we use $\mathbb{S}_{>0}^n$ and $\mathbb{S}_{\geq 0}^n$ to denote the set of real positive definite and positive semidefinite matrices. For column vectors $x \in \mathbb{R}^n$ and $y \in \mathbb{R}^m$ we define $(x, y) = [x^\top, y^\top]^\top \in \mathbb{R}^{n+m}$. Moreover, $\|x\| = \sqrt{x^\top x}$ denotes the Euclidean norm and $\|x\|_{\mathcal{C}} := \min_{z \in \mathcal{C}} \|z - x\|$ denotes the point to set distance. Furthermore, I_n , $0_{n \times m}$, 0_n , and $\mathbf{1}_n$ denote the n -dimensional identity matrix, $n \times m$ zero matrix, and column vectors of zeros and ones of length n respectively. The cardinality of a discrete set \mathcal{X} is denoted by $|\mathcal{X}|$. The Kronecker product is denoted by \otimes . We use $\varphi_x(t, x_0)$ to denote a (Carathéodory) solution of $\frac{d}{dt}x = f(x)$ at time $t \in \mathbb{R}_{\geq 0}$ starting from x_0 at time $t = 0$.

II. NETWORK MODEL AND CONVERTER CONTROL

In this section, we introduce the ac power network model, converter model, and converter control that will be considered throughout the paper.

A. Power network and converter model

Consider an ac power network modeled by a simple, connected and undirected graph $\mathcal{G} := \{\mathcal{N}, \mathcal{E}, \mathcal{W}\}$ with edge set $\mathcal{E} := \mathcal{N} \times \mathcal{N}$ corresponding to $|\mathcal{E}| = e$ transmission lines, set of nodes \mathcal{N} corresponding to $|\mathcal{N}| = n$ voltage source converters, and set of edge weights $\mathcal{W} = \{w_1, \dots, w_e\}$ with $w_i \in \mathbb{R}_{>0}$ for all $i \in \{1, \dots, e\}$. Throughout this work, we assume that the network is lossless, modeled through a Kron-reduced graph [23]. Moreover, we model each voltage source converter $i \in \mathcal{N}$ as a voltage source imposing an ac voltage with phase angle $\theta_i \in \mathbb{R}$ relative to a reference frame rotating with the nominal frequency $\omega_0 \in \mathbb{R}_{>0}$ that injects an active power denoted by $P_i \in \mathbb{R}$. Finally, for every $i \in \mathcal{N}$, we use $P_{L,i} \in \mathbb{R}$, to denote active power loads mapped from the load nodes (i.e., nodes eliminated by applying Kron reduction) to the converter nodes using Kron reduction [23].

Linearizing the (quasi-steady-state) ac power flow equation at the nominal voltage magnitude and zero angle difference between the nodes, results in the converter power injection

$$P := L\theta + P_L,$$

where $L := BWB^T$ is the Laplacian matrix of the graph \mathcal{G} , $B \in -1, 0, 1^{n \times e}$ denotes the oriented incidence matrix of \mathcal{G} [24], and $W = \text{diag}\{w_i\}_{i=1}^e$. Moreover, $\theta = (\theta_1, \dots, \theta_n) \in \mathbb{R}^n$ is the vector of ac voltage phase angles (relative to $\omega_0 t$), $P_L := (P_{L,1}, \dots, P_{L,n}) \in \mathbb{R}^n$ is the vector of active power loads at every node, and $P = (P_1, \dots, P_n) \in \mathbb{R}^n$ is the vector of converter power injections.

B. Review of droop control and power-limiting droop control

Grid-forming power-limiting droop control [16], [25] as shown in Fig. 1 uses a measurement of the converter power injection $P_i \in \mathbb{R}$ to determine the frequency $\omega_i = \frac{d}{dt}\theta_i \in \mathbb{R}$ (relative to the nominal frequency ω_0) of the ac voltage imposed by the converter at its bus $i \in \mathcal{N}$. Notably, power-limiting droop control combines the widely studied (proportional) $P-f$ droop control [5], [22], [26] with (nonlinear) PI controls that aim to maintain converter power injection $P_i \in \mathbb{R}$ within lower and upper limits $P_{\ell,i} \in \mathbb{R}$ and $P_{u,i} \in \mathbb{R}$. When

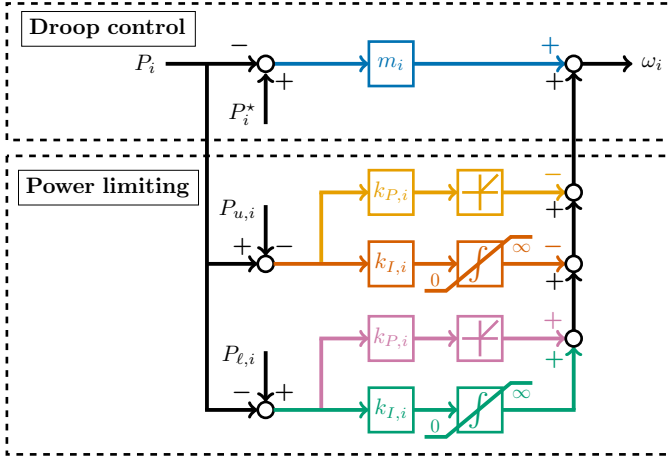


Fig. 1: Grid-forming power-limiting droop control combines droop control with nonlinear proportional-integral controls for power-limiting that activate for power-limiting when a power limit is exceeded.

no power limit is active (i.e., $P_{\ell,i} < P_i < P_{u,i}$), power-limiting droop control reduces to well-known (proportional) $P-f$ droop control [5] that controls the converter power injection [26, Sec. IV-C] by adjusting the frequency ω_i in proportion to the deviation of $P_i \in \mathbb{R}$ from the converter power setpoint $P_i^* \in \mathbb{R}$ to enable parallel operation [5] of grid-forming converters.

We emphasize that, in general, the load $P_L \in \mathbb{R}$ is not known, and the sum of the power setpoints does not match the load (i.e., $\sum_{i \in \mathcal{N}} P_i^* \neq \sum_{i \in \mathcal{N}} P_{L,i}$). Moreover, the exact topology and edge weights of the graph \mathcal{G} is generally not known. In this setting, the control objective is to render a

synchronous solution (i.e., $\omega_i = \omega_j$ for all $(i, j) \in \mathcal{N} \times \mathcal{N}$) stable for any connected graph \mathcal{G} while sharing any additional load between the converters according to the ratio of droop coefficients $m_i \in \mathbb{R}_{>0}$ (see, e.g., [22]).

While $P-f$ droop control achieves these objectives under mild assumptions [22], [27], it does not account for the converter power limits $P_{\ell,i} < P_i < P_{u,i}$. A common heuristic used to include power limits employs proportional-integral (PI) $P-f$ droop with proportional and integral gains $k_{P,i} \in \mathbb{R}_{>0}$ and $k_{I,i} \in \mathbb{R}_{>0}$ that activate when a power limit is reached [16, Fig. 4].

For example, if a converter reaches or exceeds its upper power limit (i.e., $P_i \geq P_{u,i}$), then power-limiting droop control depicted in Fig. 1 will reduce the frequency in proportion to the constraint violation and its integral. Due to the nature of integral control, this control should intuitively control the converter to an operating point within its power limits asymptotically. However, to the best of the author's knowledge, no analytical results for this control are available in the literature. The main contribution of this work is to begin to close this gap and show that, under mild assumptions, power-limiting droop control renders the overall converter-based system stable with respect to a synchronous solution within the converter power limits.

To ensure that the control and analysis problem is well-posed, we first formalize the following assumptions that are implicitly made in the literature.

Assumption 1 (Feasible power limits and load) For all $i \in \mathcal{N}$, the power limits $P_{\ell,i} \in \mathbb{R}^n$ and $P_{u,i} \in \mathbb{R}^n$ satisfy $P_{\ell,i} < P_{u,i}$. Moreover, the load $P_L \in \mathbb{R}^n$ satisfies $\sum_{i=1}^n P_{\ell,i} < \sum_{i=1}^n P_{L,i} < \sum_{i=1}^n P_{u,i}$.

Assumption 2 (Feasible power setpoints) The power setpoints $P_i^* \in \mathbb{R}^n$ satisfy $P_{\ell,i} < P_i^* < P_{u,i}$.

C. Power system dynamics as projected dynamical system

We begin by formulating the frequency dynamics of a power system comprised of converters using power-limiting droop control as a projected dynamical system. To this end, we introduce the tangent cone and the projection operator.

Definition 1 (Normal and tangent cone) Given a non-empty convex set $\mathcal{C} \subseteq \mathbb{R}^n$, and a point $x \in \mathcal{C}$, the normal cone $\mathcal{N}_x \mathcal{C}$ is given by

$$\mathcal{N}_x \mathcal{C} := \{w \in \mathbb{R}^n \mid w^T(x' - x) \leq 0, \quad \forall x' \in \mathcal{C}\}.$$

Then, the tangent cone of the set \mathcal{C} at the point x is defined as the polar cone of the normal cone

$$\mathcal{T}_x \mathcal{C} := \{v \in \mathbb{R}^n \mid v^T w \leq 0, \quad \forall w \in \mathcal{N}_x \mathcal{C}\}.$$

Next, we define the projection operator.

Definition 2 (Projection) Given a convex set $\mathcal{C} \subseteq \mathbb{R}^n$ and a vector $v \in \mathbb{R}^n$, $\Pi_{\mathcal{C}}(v)$ denotes the projection of v with respect to the set \mathcal{C} , i.e., $\Pi_{\mathcal{C}}(v) = \operatorname{argmin}_{p \in \mathcal{C}} \|p - v\|$.

Broadly speaking, projecting a dynamical system $\frac{d}{dt}x = f(x)$ onto a set \mathcal{C} results in the projected dynamical system

$\frac{d}{dt}x = \Pi_{\mathcal{T}_x} \mathcal{C}(f(x))$ that does not leave the set \mathcal{C} [28]. While inherently discontinuous, strong theoretical results on the stability and convergence properties of projected dynamical systems are available in the literature (see, e.g., [29]).

We now use Definition 1 and Definition 2 to express power-limiting droop control for each converter $i \in \mathcal{N}$ as the projected dynamical system

$$\frac{d}{dt}\theta_i = m_i(P_i^* - P_i) - k_{P,i}\Pi_{\mathbb{R}_{\geq 0}}(P_i - P_{u,i}) - \mu_{u,i} \quad (1a)$$

$$+ k_{P,i}\Pi_{\mathbb{R}_{\geq 0}}(P_{\ell,i} - P_i) + \mu_{\ell,i},$$

$$\frac{d}{dt}\mu_{\ell,i} = \Pi_{\mathcal{T}_{\mu_{\ell,i}}\mathbb{R}_{\geq 0}}(k_{I,i}(P_{\ell,i} - P_i)), \quad (1b)$$

$$\frac{d}{dt}\mu_{u,i} = \Pi_{\mathcal{T}_{\mu_{u,i}}\mathbb{R}_{\geq 0}}(k_{I,i}(P_i - P_{u,i})), \quad (1c)$$

with controller states $\theta_i, \mu_{u,i} \in \mathbb{R}_{\geq 0}$, and $\mu_{\ell,i} \in \mathbb{R}_{\geq 0}$ that correspond to the ac voltage phase angles and integral of the upper and lower power limit violations. Moreover, we define the ac voltage frequency deviation $\omega_i = \frac{d}{dt}\theta_i \in \mathbb{R}$ from the nominal frequency ω_0 .

To simplify our analysis and notation, we introduce the following preliminary result.

Lemma 1 (Scaled scalar projection) *Given a constant $a \in \mathbb{R}_{>0}$ and scalars $v \in \mathbb{R}$ and $x \in \mathbb{R}$, it holds that $\Pi_{\mathcal{T}_x\mathbb{R}_{\geq 0}}(av) = a\Pi_{\mathcal{T}_x\mathbb{R}_{\geq 0}}(v)$.*

Proof. Using [30, Prop. 5.3.5], $\Pi_{\mathcal{T}_x\mathbb{R}_{\geq 0}}(v)$ can be expressed as $\Pi_{\mathcal{T}_x\mathcal{C}}(v) = \lim_{\delta \rightarrow 0} \frac{1}{\delta}(\Pi_{\mathcal{C}}(x + \delta v) - x)$. Then, for $x \in \partial(\mathcal{C})$ it holds that $\Pi_{\mathcal{T}_x\mathbb{R}_{\geq 0}}(av) = \lim_{\delta \rightarrow 0} \frac{1}{\delta}(\Pi_{\mathbb{R}_{\geq 0}}(x + \delta av) - x)$. Letting $\delta' = a\delta$ results in $\Pi_{\mathcal{T}_x\mathbb{R}_{\geq 0}}(av) = a \lim_{\delta' \rightarrow 0} \frac{1}{\delta'}(\Pi_{\mathbb{R}_{\geq 0}}(x + \delta'v) - x) = a\Pi_{\mathcal{T}_x\mathbb{R}_{\geq 0}}(v)$. \square

Using Lemma 1, we can rewrite (1) using the change of variables $\sqrt{k_{I,i}}\lambda_{\ell,i} = \mu_{\ell,i}$, and $\sqrt{k_{I,i}}\lambda_{u,i} = \mu_{u,i}$ as

$$\frac{d}{dt}\theta_i = m_i(P_i^* - P_i) - k_{P,i}\Pi_{\mathbb{R}_{\geq 0}}(P_i - P_{u,i}) \quad (2a)$$

$$+ k_{P,i}\Pi_{\mathbb{R}_{\geq 0}}(P_{\ell,i} - P_i) - \sqrt{k_{I,i}}(\lambda_{u,i} - \lambda_{\ell,i}),$$

$$\frac{d}{dt}\lambda_{\ell,i} = \Pi_{\mathcal{T}_{\lambda_{\ell,i}}\mathbb{R}_{\geq 0}}\left(\sqrt{k_{I,i}}(P_{\ell,i} - P_i)\right), \quad (2b)$$

$$\frac{d}{dt}\lambda_{u,i} = \Pi_{\mathcal{T}_{\lambda_{u,i}}\mathbb{R}_{\geq 0}}\left(\sqrt{k_{I,i}}(P_i - P_{u,i})\right). \quad (2c)$$

To obtain the overall power system dynamics, we introduce the vector of power setpoints $P^* := (P_1^*, \dots, P_n^*) \in \mathbb{R}^n$, vectors $P_{\ell} := (P_{\ell,1}, \dots, P_{\ell,n}) \in \mathbb{R}^n$ and $P_u := (P_{u,1}, \dots, P_{u,n}) \in \mathbb{R}^n$ collecting lower and upper power limits, as well as vectors $\lambda_u = (\lambda_{u,1}, \dots, \lambda_{u,n}) \in \mathbb{R}_{\geq 0}^n$ and $\lambda_{\ell} = (\lambda_{\ell,1}, \dots, \lambda_{\ell,n}) \in \mathbb{R}_{\geq 0}^n$ collecting the integrator states. Moreover, the matrices $M := \text{diag}\{m_i\}_{i=1}^n \in \mathbb{S}_{>0}^n$, $K_P := \text{diag}\{k_{P,i}\}_{i=1}^n$, and $K_I := \text{diag}\{\sqrt{k_{I,i}}\}_{i=1}^n$ collect the droop coefficients $m_i \in \mathbb{R}_{>0}$, proportional gains $k_{P,i} \in \mathbb{R}_{>0}$, and square root of the integral gains $k_{I,i} \in \mathbb{R}_{>0}$. Vectorizing (2) and substituting (1a), the frequency dynamics of a multi-converter system using power-limiting droop control are given by

$$\frac{d}{dt}\theta = M(P^* - P_L - L\theta) - (\alpha \otimes K_I)\lambda \quad (3a)$$

$$- (\alpha \otimes K_P)\Pi_{\mathbb{R}_{\geq 0}^{2n}}(g(L\theta)),$$

$$\frac{d}{dt}\lambda = \Pi_{\mathcal{T}_{\lambda}\mathbb{R}_{\geq 0}^{2n}}((I_2 \otimes K_I)g(L\theta)), \quad (3b)$$

where $\alpha := (-1, 1)^T$, $\lambda := (\lambda_{\ell}, \lambda_u) \in \mathbb{R}_{\geq 0}^{2n}$, and the function $g: \mathbb{R}^n \rightarrow \mathbb{R}^{2n}$ and network power injection $P_N := L\theta$ are

used to express the violation of power limits as

$$g(P_N) := \begin{bmatrix} P_{\ell} - P_N - P_L \\ P_N + P_L - P_u \end{bmatrix}.$$

We emphasize that this model assumes that the load P_L , power setpoints P^* , and power limits P_{ℓ} and P_u are constant. This assumption is satisfied on the time-scales of interest for studying frequency stability of converter-dominated power systems. Extensions to time-varying loads, setpoints, and power limits are seen as an interesting area for future work.

III. STABILITY OF POWER-LIMITING DROOP CONTROL

In this section, we introduce a constrained dc power flow (CDCPF) problem and characterize its optimizers. Moreover, we present the main result of this work that establishes that the multi-converter system (3) is globally asymptotically stable with respect to a solution of the constrained power flow problem. A detailed analysis and proof of the main result will be presented in subsequent sections.

A. Constrained dc power flow problem in nodal coordinates

Consider the constrained dc power flow (CDCPF) problem

$$\min_{\theta} \frac{1}{2}(P - P^*)^T M (P - P^*) \quad (4a)$$

$$\text{s.t. } P_{\ell} \leq P \leq P_u \quad (4b)$$

$$P = L\theta + P_L \quad (4c)$$

that seeks optimal angles $\theta^* \in \mathbb{R}^n$ (i.e., nodal variables) that minimize the cost of deviating from the power setpoint $P^* \in \mathbb{R}^n$ subject to the converter power limits $P_{\ell} \in \mathbb{R}^n$ and $P_u \in \mathbb{R}^n$ and supplying the load P_L .

We require the following preliminary result that ensures feasibility of the constrained power flow problem (4) under Assumption 1.

Proposition 1 (Feasibility in nodal coordinates) *There exists $\theta \in \mathbb{R}^n$ such that $P_{\ell} < L\theta + P_L < P_u$ if and only if P_{ℓ}, P_u , and P_L satisfy Assumption 1.*

Proof. Under Assumption 1, there exists $P_f \in \mathbb{R}^n$ such that $P_{\ell} < P_f < P_u$ and $\mathbb{1}_n^T P_f = \mathbb{1}_n^T P_L$. Next, we note that there exists $\theta \in \mathbb{R}^n$ such that $P_f - P_L = L\theta$ if and only if $(P_f - P_L) \perp \mathbb{1}_n$ [24, Lem. 6.12] or, equivalently, if and only if $\mathbb{1}_n^T(P_f - P_L) = 0$ and sufficiency of Assumption 1 immediately follows. Next, note that there only exists $\theta \in \mathbb{R}^n$ such that $P_{\ell} < L\theta + P_L < P_u$ if $\mathbb{1}_n^T P_{\ell} < \mathbb{1}_n^T(L\theta + P_L) < \mathbb{1}_n^T P_u$. Using $\mathbb{1}_n^T L = 0$, it directly follows that $\sum_{i=1}^n P_{\ell,i} < \sum_{i=1}^n P_L,i < \sum_{i=1}^n P_{u,i}$ is necessary. \square

Making the constraint (4c) explicit, scaling the constraint (4b) by the diagonal matrix $K_I \in \mathbb{S}_{>0}^n$, expanding the cost function, and dropping constant terms that do not depend on θ , it can be shown that the optimizer of (4) is equivalent to the optimizer of

$$\min_{\theta} \frac{1}{2}\theta^T L M L \theta + (P_L - P^*)^T M L \theta \quad (5a)$$

$$\text{s.t. } K_I P_{\ell} \leq K_I(L\theta + P_L) \leq K_I P_u. \quad (5b)$$

Next, we define the set of points that satisfy the Karush-Kuhn-Tucker (KKT) [31, Ch. 5] conditions of (5). Note that the stationary condition requires

$$L(M(L\theta^* + P_L - P^*) + K_I(\lambda_u^* - \lambda_\ell^*)) = \mathbf{0}_n.$$

Then, using $\ker(L) = \ker(B^\top)$, we can express the KKT conditions as follows.

Definition 3 (KKT points in nodal coordinates) $\mathcal{S}_\theta \subseteq \mathbb{R}^{3n}$ denotes the set of points $(\theta^*, \lambda_\ell^*, \lambda_u^*)$ that satisfy the KKT conditions of the CDCPF in nodal coordinates (5), i.e., $P_\ell \leq L\theta^* + P_L \leq P_u$, $(\lambda_\ell^*, \lambda_u^*) \in \mathbb{R}_{\geq 0}^{2n}$, and

$$M(L\theta^* + P_L - P^*) + K_I(\lambda_u^* - \lambda_\ell^*) \in \ker B^\top, \quad (6a)$$

$$\text{diag}\{\lambda_{\ell,i}^*\}_{i=1}^n K_I(P_\ell - L\theta^* - P_L) = \mathbf{0}_n, \quad (6b)$$

$$\text{diag}\{\lambda_{u,i}^*\}_{i=1}^n K_I(L\theta^* + P_L - P_u) = \mathbf{0}_n. \quad (6c)$$

The next property directly follows from $\ker L = \mathbb{1}_n$ and formalizes that KKT points of (4) are not unique or isolated.

Property 1 (Non-unique KKT points) For any $(\theta^*, \lambda^*) \in \mathcal{S}_\theta$ and all $c \in \mathbb{R}$ it holds that $(\theta^* + c\mathbf{1}_n, \lambda^*) \in \mathcal{S}_\theta$.

B. Stability of constrained systems with respect to a set

Before stating our main result, we require the following definition of a forward invariant set.

Definition 4 (Forward invariant set) A set \mathcal{D} is called forward invariant under the dynamics $\frac{d}{dt}x = f(x)$ if, for any $x_0 \in \mathcal{D}$, it holds that $\varphi_x(t, x_0) \in \mathcal{D}$ for all $t \in \mathbb{R}_{>0}$.

In other words, Definition 4 requires that the solution $\varphi_x(t, x_0)$ of a dynamical system remains in \mathcal{D} for all times if the initial condition x_0 is in \mathcal{D} . Moreover, we require the following definition of stability with respect to a set.

Definition 5 (Asymptotic stability with respect to a set) Given a dynamic system $\frac{d}{dt}x = f(x)$ and forward invariant set \mathcal{D} , $\frac{d}{dt}x = f(x)$ is called globally asymptotically stable with respect to a set $\mathcal{C} \subseteq \mathcal{D}$ in \mathcal{D} if

- (i) it is almost globally attractive with respect to \mathcal{C} , i.e., $\lim_{t \rightarrow \infty} \|\varphi(t, x_0)\|_{\mathcal{C}} = 0$ holds for all $x_0 \in \mathcal{D}$, and
- (ii) it is Lyapunov stable with respect to \mathcal{C} , i.e., for every $\varepsilon \in \mathbb{R}_{>0}$ there exists $\delta \in \mathbb{R}_{>0}$ such that $x_0 \in \mathcal{D}$ and $\|x_0\|_{\mathcal{C}} < \delta$ implies $\|\varphi(t, x_0)\|_{\mathcal{C}} < \varepsilon$ for all $t \in \mathbb{R}_{\geq 0}$.

Notably, the definition of asymptotic stability typically assumes compactness of the set \mathcal{C} [32]. Because Definition 5 does not require \mathcal{C} to be compact, stability with respect to \mathcal{C} does not necessarily imply convergence to a limit cycle or an equilibrium, but trajectories may tend to infinity within the set \mathcal{C} . In the application at hand, the dynamics not bounded by \mathcal{C} correspond to the synchronous frequency dynamics upon convergence, which we will study separately.

Using standard arguments (see [33], [34, Ch. VI]) one can show that Definition 5 is identical to the following condition.

Definition 6 (Comparison functions) A function $\chi : \mathbb{R}_{\geq 0} \rightarrow \mathbb{R}_{\geq 0}$ is of class \mathcal{K} if it is continuous, strictly increasing and $\chi(0) = 0$. A function $\chi : \mathbb{R}_{\geq 0} \rightarrow \mathbb{R}_{>0}$ is of class \mathcal{L} if it is continuous, non-increasing, and $\chi(s) \rightarrow 0$ as $s \rightarrow \infty$.

Condition 1 (Comparison function characterization) Consider a function $\chi(\|x_0\|_{\mathcal{C}}, t) \in \mathcal{K}\mathcal{L}$, i.e., it is of class \mathcal{K} in its first argument and class \mathcal{L} in its second argument. Asymptotic stability with respect to \mathcal{C} in \mathcal{D} is equivalent to

$$\|\varphi_x(t, x_0)\|_{\mathcal{C}} \leq \chi(\|x_0\|_{\mathcal{C}}, t), \quad \forall x_0 \in \mathcal{D}, \forall t \in \mathbb{R}_{\geq 0}.$$

If $\mathcal{D} = \mathbb{R}^n$, then Definition 5 implies global asymptotic stability. For the system (3), $\mathcal{D} = \mathbb{R}^n \times \mathbb{R}_{\geq 0}^{2n} \neq \mathbb{R}^n$ but contains all initial conditions. Thus, with a slight abuse in terminology, we will refer to the system as globally asymptotically stable for $\mathcal{D} = \mathbb{R}^n \times \mathbb{R}_{\geq 0}^{2n}$.

C. Summary of main results

We are now ready to state our main stability result.

Theorem 1 (Global asymptotic stability) Consider P_ℓ , P_u , P_L , and P^* such that Assumption 1 and Assumption 2 hold. For any connected graph \mathcal{G} , (3) is globally asymptotically stable on $\mathbb{R}^n \times \mathbb{R}_{\geq 0}^{2n}$ with respect to the set \mathcal{S}_θ . Moreover, there exists a synchronous frequency $\omega_s \in \mathbb{R}$ such that $\lim_{t \rightarrow \infty} \omega_i(t) = \omega_s$ for all $i \in \mathcal{N}$.

A proof is provided in Section IV. Theorem 1 shows that (3) is Lyapunov stable with respect to the set \mathcal{S}_θ of KKT points of the CDCPF (5) and converges to an optimizer in \mathcal{S}_θ as $t \rightarrow \infty$. Notably, by Property 1 this implies that (3) is globally asymptotically stable with respect to a synchronous solution but not necessarily with respect to an equilibrium point.

We require the following definition to further characterize the synchronous solutions in the set \mathcal{S}_θ .

Definition 7 (Active constraint sets) We define $\mathcal{I}_\ell \subseteq \mathcal{N}$ and $\mathcal{I}_u \subseteq \mathcal{N} \setminus \mathcal{I}_\ell$ as the set of converters operating at their lower and upper power limit, i.e., $i \in \mathcal{I}_\ell$ if and only if $P_i = P_{\ell,i}$ and $i \in \mathcal{I}_u$ if and only if $P_i = P_{u,i}$.

Next, we establish that (3) converges to a synchronous frequency $\omega_s \in \mathbb{R}$ and we characterize the synchronous frequency ω_s as a function of the total load $\sum_{i \in \mathcal{N}} P_{L,i}$, total power dispatch $\sum_{i \in \mathcal{N}} P_i^*$, and active sets \mathcal{I}_u and \mathcal{I}_ℓ .

Theorem 2 (Frequency synchronization) Consider P_ℓ , P_u , P_L , and P^* such that Assumption 1 and Assumption 2 hold. One of the following holds

- (i) $\sum_{i \in \mathcal{N}} P_{L,i} < \sum_{i \in \mathcal{N}} P_i^*$ and

$$\omega_s = \frac{\sum_{i \notin \mathcal{I}_\ell} P_i^* + \sum_{i \in \mathcal{I}_\ell} P_{\ell,i} - \sum_{i \in \mathcal{N}} P_{L,i}}{\sum_{i \notin \mathcal{I}_\ell} m_i^{-1}} > 0,$$

- (ii) $\sum_{i \in \mathcal{N}} P_{L,i} = \sum_{i \in \mathcal{N}} P_i^*$ and $\omega_s = 0$,
- (iii) $\sum_{i \in \mathcal{N}} P_{L,i} > \sum_{i \in \mathcal{N}} P_i^*$ and

$$\omega_s = \frac{\sum_{i \notin \mathcal{I}_u} P_i^* + \sum_{i \in \mathcal{I}_u} P_{u,i} - \sum_{i \in \mathcal{N}} P_{L,i}}{\sum_{i \notin \mathcal{I}_u} m_i^{-1}} < 0.$$

A proof is provided in Section IV. Moreover, the following Corollary that characterizes the active constraint set is an immediate consequence of Theorem 2.

Corollary 1 (Active constraint set) Consider P_ℓ , P_u , P_L , and P^* such that Assumption 1 and Assumption 2 hold. Then, for all $(\theta, \lambda) \in \mathcal{S}_\theta$ it holds that

- (i) $\mathcal{I}_\ell \neq \emptyset$ implies $\mathcal{I}_u = \emptyset$ and $\sum_{i \in \mathcal{N}} P_{L,i} < \sum_{i \in \mathcal{N}} P_i^*$,
- (ii) $\mathcal{I}_u \neq \emptyset$ implies $\mathcal{I}_\ell = \emptyset$ and $\sum_{i \in \mathcal{N}} P_{L,i} > \sum_{i \in \mathcal{N}} P_i^*$,
- (iii) $\sum_{i \in \mathcal{N}} P_{L,i} < \sum_{i \in \mathcal{N}} P_i^*$ implies $\mathcal{I}_u = \emptyset$,
- (iv) $\sum_{i \in \mathcal{N}} P_{L,i} > \sum_{i \in \mathcal{N}} P_i^*$ implies $\mathcal{I}_\ell = \emptyset$.

In particular, Theorem 2 recovers and extends the well known results for (proportional) $P-f$ droop control, i.e., if no converter is operating at a power limit (i.e., $\mathcal{I}_u = \mathcal{I}_\ell = \emptyset$), then the steady-state frequency deviation is determined by the droop coefficients $m_i \in \mathbb{R}_{>0}$ and the mismatch $\sum_{i \in \mathcal{N}} P_i^* - P_{L,i}$ between the total power dispatch and load.

Moreover, if the total load $\sum_{i \in \mathcal{N}} P_{L,i}$ is smaller than the total power dispatch $\sum_{i \in \mathcal{N}} P_i^*$, then converters can only be at their lower power limit (i.e., $\mathcal{I}_u = \emptyset$) and the synchronous frequency is determined by the sum of the droop coefficients and sum of the power setpoints of converters not at the lower limit (i.e., $i \notin \mathcal{I}_\ell$), the total load, and the sum of the lower power limits of the converters at the lower limit (i.e., $i \in \mathcal{I}_\ell$). In contrast, if the total load $\sum_{i \in \mathcal{N}} P_{L,i}$ is larger than the total power dispatch $\sum_{i \in \mathcal{N}} P_i^*$, then converters can only be at their upper power limit (i.e., $\mathcal{I}_\ell = \emptyset$) and the synchronous frequency is determined by the sum of the droop coefficients and sum of the power setpoints of converters not at the upper limit (i.e., $i \notin \mathcal{I}_u$), the total load, and the sum of the upper power limits of the converters at the upper limit (i.e., $i \in \mathcal{I}_u$).

Moreover, we note that if $\sum_{i \in \mathcal{N}} P_{L,i}$ is smaller (larger) than the total power dispatch $\sum_{i \in \mathcal{N}} P_i^*$, then the synchronous frequency is larger (smaller) than nominal frequency ω_0 . The remainder of the manuscript will focus on proving the aforementioned results.

Finally, the next result formalizes that, upon convergence to \mathcal{S}_θ , if any converter is operating at the upper power limit, no converter can operate at the lower power limit and vice versa.

Proposition 2 (Mutually exclusive active sets) Consider P_ℓ , P_u , P_L , and P^* such that Assumption 1 and Assumption 2 hold. Then, for all $(\theta, \lambda) \in \mathcal{S}_\theta$, either $\mathcal{I}_\ell = \emptyset$ or $\mathcal{I}_u = \emptyset$.

A proof is provided in Section IV.

IV. STABILITY ANALYSIS OF POWER-LIMITING DROOP CONTROL

In this section, we present the stability analysis and proofs that establish our main results stated in the previous section.

A. Overview and proof strategy

To establish the equivalence between the CDCPF (4) and dynamics of the converter-based power system using power-limiting droop control (3) we will use the proof strategy shown in Fig. 2. Our results crucially depend on two main steps. First, we use the oriented incidence matrix B and decomposition $V \in \mathbb{R}^{e \times e}$ of the weight matrix $W = VV \in \mathbb{R}^{e \times e}$ of the graph \mathcal{G} to define the change of coordinates $\eta = VB^\top \theta$. Notably, this change of coordinates transforms nodal angles to angle differences across graph edges (i.e., transmission lines).

Applying this change of coordinates to the CDCPF (4) results in an optimization problem in edge coordinates whose KKT points can be related to the KKT points of the CDCPF (4) under the restriction $V \in \text{Im}(B^\top)$.

Second, we show that, in edge coordinates η , a network of converters using power-limiting droop control (3) can be interpreted as a distributed primal-dual algorithm solving (4) while maintaining $\eta(t) \in \text{Im}(VB^\top)$ for all times $t \in \mathbb{R}_{\geq 0}$ if $\eta(0) \in \text{Im}(VB^\top)$. Notably, the dynamics in edge coordinates can be decomposed into dynamics associated with primal-dual dynamics resulting from a strictly convex problem and remaining dynamics that are stable in the sense of Lyapunov. The primal-dual dynamics resulting from a strictly convex problem can then be analyzed using well-known results from [17].

Combining the aforementioned results allows us to establish that (3) is globally asymptotically stable with respect to the set of KKT points of the constrained dc power flow problem (4). Moreover, we will use properties of the set of KKT points to establish that (3) achieves frequency synchronization under constraints and establish that the synchronous frequency deviation is a function of the active constraint set, load, power setpoints, and droop coefficients, but does not depend on the graph \mathcal{G} or the control gains of the power-limiting PI controls.

B. Constrained dc power flow problem in edge coordinates

To establish our main result, we reformulate the constrained dc power flow problem (4) in edge coordinates. To this end, consider the (weighted) angle differences $\eta := VB^\top \theta \in \mathbb{R}^e$ between connected converters and the decomposition

$$L\theta = BVVB^\top \theta = BV\eta \quad (7)$$

of the Laplacian matrix L into its oriented incidence matrix $B \in \mathbb{R}^{n \times e}$ and weight matrix $V := W^{\frac{1}{2}} \in \mathbb{R}^{e \times e}$. Applying (7) to (5) results in the constrained DCPF problem in edge coordinates

$$\min_{\eta} \frac{1}{2} \eta^\top VB^\top MBV\eta + (P_L - P^*)^\top MBV\eta \quad (8a)$$

$$\text{s.t. } K_I P_\ell \leq K_I (BV\eta + P_L) \leq K_I P_u. \quad (8b)$$

Notably, the Hessian $VB^\top MBV \in \mathbb{S}_{>0}^e$ of (8) becomes a weighted edge Laplacian matrix (see [21], [35] for details) if $M = cI_e$ for some $c \in \mathbb{R}_{>0}$. We will show that $VB^\top MBV \in \mathbb{S}_{>0}^e$ (i.e., (8) is strongly convex) when \mathcal{G} has no cycles but $VB^\top MBV \in \mathbb{S}_{\geq 0}^e$ otherwise. In other words, $\eta = VB^\top \theta$ is not a similarity transform for power systems with meshed topology. Before investigating this aspect further, the same steps as in the proof of Proposition 1 can be used to show that (8) admits a feasible solution under Assumption 1.

Proposition 3 (Feasibility in edge coordinates) There exists $\eta \in \mathbb{R}^e$ such that $P_\ell < BV\eta + P_L < P_u$ if and only if P_ℓ , P_u , and P_L satisfy Assumption 1.

Next, we characterize the optimizers of (8). Note that the stationary condition requires

$$B^\top (M(BV\eta^* + P_L - P^*) + K_I(\lambda_u^* - \lambda_\ell^*)) = \mathbb{0}_e.$$

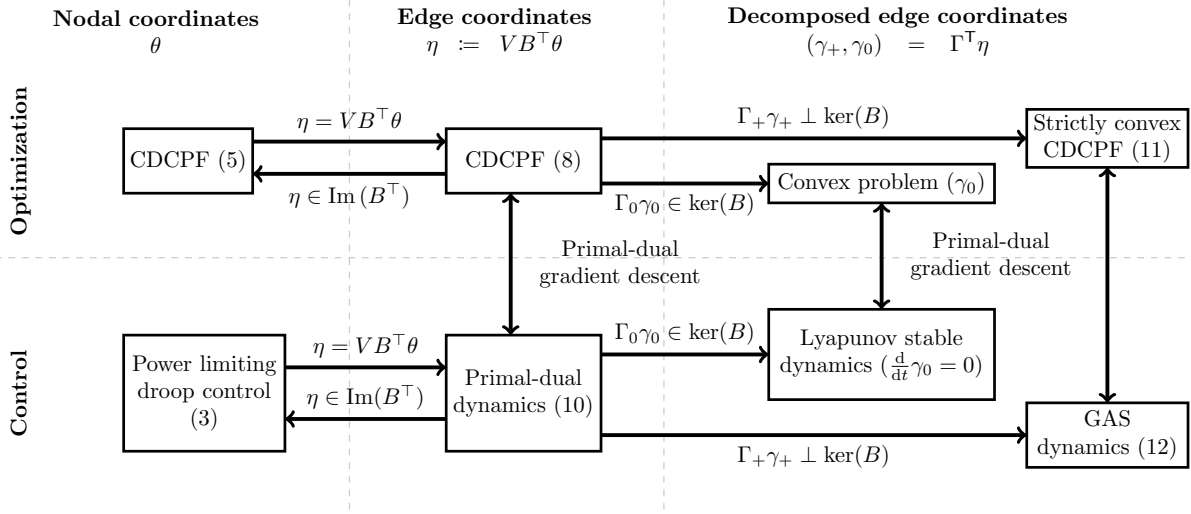


Fig. 2: The dynamics of the converter-based power system using power-limiting droop control in edge coordinates coincide with the primal-dual dynamics associated of the CDCPF in edge coordinates. To establish our main result, we show that the dynamics in edge and node coordinates are identical up to the dynamics of $\eta \in \ker(B^T)$.

Thus, the KKT conditions can be expressed as follows.

Definition 8 (KKT points of CDCPF in edge coordinates) $\mathcal{S}_\eta \subseteq \mathbb{R}^{e+2n}$ denotes the set of points $(\eta^*, \lambda_\ell^*, \lambda_u^*)$ that satisfy the KKT conditions of the CDCPF in edge coordinates (8), i.e., $P_\ell \leq BV\eta^* + P_L \leq P_u$, $(\lambda_\ell^*, \lambda_u^*) \in \mathbb{R}_{\geq 0}^{2n}$, and

$$M(BV\eta^* + P_L - P^*) + K_I(\lambda_u^* - \lambda_\ell^*) \in \ker(B^T), \quad (9a)$$

$$\text{diag}\{\lambda_{u,i}^*\}_{i=1}^n K_I(BV\eta^* + P_L - P_u) = \mathbf{0}_n, \quad (9b)$$

$$\text{diag}\{\lambda_{\ell,i}^*\}_{i=1}^n K_I(P_\ell - BV\eta^* - P_L) = \mathbf{0}_n. \quad (9c)$$

The following result clarifies the relationship between KKT points of the constrained power flow problem (4) in nodal coordinates and the constrained power flow problem (8) in edge coordinates.

Proposition 4 (KKT points in edge coordinates)

- (i) For any $(\eta^*, \lambda^*) \in \mathcal{S}_\eta$, there exist $\theta^* = VB^T\eta^*$ such that $(\theta^*, \lambda^*) \in \mathcal{S}_\theta$ if and only if $\eta^* \in \text{Im}(B^T)$.
- (ii) $(\theta^*, \lambda^*) \in \mathcal{S}_\theta$ if and only if $(VB^T\theta^*, \lambda^*) \in \mathcal{S}_\eta$.

Proof. Note that $\theta^* \in \mathbb{R}^n$ such that $\theta^* = VB^T\eta^*$ exists if and only if $\eta^* \in \text{Im}(B^T)$. Then, the first statement immediately follows by substituting $\theta^* = VB^T\eta^*$ into the equations defining \mathcal{S}_θ and noting that $\ker(L) = \ker(B^T)$. To show the second statement, substitute $(\eta^*, \lambda^*) = (VB^T\theta^*, \lambda^*)$ into (9). Then, both $(\theta^*, \lambda^*) \in \mathcal{S}_\theta$ and $(VB^T\theta^*, \lambda^*) \in \mathcal{S}_\eta$ hold if and only if $M(L\theta^* + P_L + P^*) + K_I(\lambda_u^* - \lambda_\ell^*) \in \ker(B^T)$. \square

In other words, $\eta^* \in \text{Im}(VB^T)$ ensures that the angle differences $\eta^* \in \mathbb{R}^e$ are restricted to the set $\text{Im}(B^T)$ for which a corresponding angle configuration $\theta^* \in \mathbb{R}^n$ can be found. Moreover, the sets of KKT points of (4) and (8) coincide under the edge transformation $\eta = VB^T\theta$.

C. Constrained primal-dual dynamics in edge coordinates

Next, we will investigate stability of primal-dual gradient descent applied to the CDCPF in edge coordinates (8). The

augmented Lagrangian associated with (8) is given by

$$\begin{aligned} \mathcal{L}(\eta, \lambda) := & \frac{1}{2}\eta^T VB^T MBV\eta + (P_L - P^*)^T MBV\eta \\ & + \frac{1}{2} \left[\Pi_{\mathbb{R}_{\geq 0}^{2n}}(g(BV\eta)) \right]^T (I_2 \otimes K_P) \Pi_{\mathbb{R}_{\geq 0}^{2n}}(g(BV\eta)) \\ & + \lambda^T K_I g(BV\eta), \end{aligned}$$

Next, we introduce the primal-dual gradient dynamics $\frac{d}{dt}\eta = -\nabla_\eta \mathcal{L}$, $\frac{d}{dt}\lambda = \Pi_{\mathcal{T}_{\lambda} \mathbb{R}_{\geq 0}^{2n}}(\nabla_\lambda \mathcal{L})$ associated with the augmented Lagrangian. This results in

$$\begin{aligned} \frac{d}{dt}\eta = & VB^T(M(P^* - P_L - BV\eta) - (\alpha \otimes K_I)\lambda, \\ & - (\alpha \otimes K_P) \Pi_{\mathbb{R}_{\geq 0}^{2n}}(g(BV\eta))), \end{aligned} \quad (10a)$$

$$\frac{d}{dt}\lambda = \Pi_{\mathcal{T}_{\lambda} \mathbb{R}_{\geq 0}^{2n}}((I_2 \otimes K_I)g(BV\eta)). \quad (10b)$$

The next theorem shows the primal-dual dynamics (10) are globally asymptotically stable with respect to the set of KKT points \mathcal{S}_η . In addition, we show that the primal-dual dynamics (10) converge to an equilibrium.

Theorem 3 (Global asymptotic stability of primal-dual dynamics in edge coordinates) Consider P_ℓ , P_u , P_L , and P^* such that Assumption 1 and Assumption 2 hold. Then the primal-dual dynamics (10) are globally asymptotically stable with respect to \mathcal{S}_η on $\mathbb{R}^e \times \mathbb{R}_{\geq 0}^{2n}$. Moreover, $\frac{d}{dt}(\eta, \lambda) = \mathbf{0}_{e+2n}$ holds on \mathcal{S}_η .

Proof. We begin by noting that $M \in \mathbb{S}_{>0}^n$. Then, by [36, Observation 7.1.8], $B^T MB \in \mathbb{S}_{>0}^{e \times e}$ if and only if $\text{rank } B = e$. If \mathcal{G} is a connected tree, then $n = e + 1$ and by [24, Lemma 9.2], $\text{rank } B = e$. Conversely, if \mathcal{G} contains cycles, then $e \geq n$ and $\text{rank } B \leq e - 1$. Thus, if \mathcal{G} is a tree, then the cost function of (8) is strictly convex and \mathcal{S}_η is a singleton. Moreover, by Proposition 3 there exists η such that $P_\ell < BV\eta + P_L < P_u$, i.e., Slater's condition holds. Then, [17, Theorem 4.5] immediately implies that (10) is globally asymptotically stable with respect to \mathcal{S}_η .

When \mathcal{G} contains cycles, we can decompose (8) and (10) into a strongly convex part and remaining dynamics. To this

end, let $\Gamma := [\Gamma_+ \ \Gamma_0]$ where $\Gamma_+ \in \mathbb{R}^{e \times n-1}$ contains eigenvectors corresponding to the positive eigenvalues of VB^TMBV and $\Gamma_0 \in \mathbb{R}^{e \times e-(n-1)}$ contains the eigenvectors corresponding to the zero eigenvalues. Next, let $\gamma = (\gamma_+, \gamma_0) \in \mathbb{R}^e$. Since $B^TMB \in \mathbb{S}_{\geq 0}^n$, we conclude that $\Gamma^{-1} = \Gamma^T$. Applying the change of coordinates $\eta = \Gamma\gamma$ to (8) results in

$$\min_{\eta} \frac{1}{2} \gamma_+^T H \gamma_+ + c^T \gamma_+ \quad (11a)$$

$$\text{s.t. } K_I P_\ell \leq K_I (A \gamma_+ + P_L) \leq K_I P_u, \quad (11b)$$

where $H := \Gamma_+^T VB^T MBV \Gamma_+$, $c := \Gamma_+^T VB^T MBM(P^* - P_L)$, and $A := BV \Gamma_+$. Notably, this transformation only removed redundant degrees of freedom and, by construction, (11) is strongly convex and strictly feasible under the same conditions as (8). Moreover, given a KKT point (γ_+^*, λ^*) of (11), $BV \Gamma_0 \in \mathbb{R}^{n \times e-(n-1)}$ implies that $(\Gamma_+ \gamma_+^* + \Gamma_0 \gamma_0, \lambda^*) \in \mathcal{S}_\eta$ for all $\gamma_0 \in \mathbb{R}^{e-(n-1)}$. Applying the change of coordinates $\eta = \Gamma\gamma$ to (10) results in $\frac{d}{dt} \gamma_0 = 0$ and

$$\begin{aligned} \frac{d}{dt} \gamma_+ &= -H \gamma_+ - c - \Gamma_+^T ((\alpha \otimes K_P) \Pi_{\mathbb{R}_{\geq 0}^{2n}}(g(A \gamma_+)) \\ &\quad + (\alpha \otimes K_I) \lambda), \end{aligned} \quad (12a)$$

$$\frac{d}{dt} \lambda = \Pi_{\mathcal{T}_\lambda \mathbb{R}_{\geq 0}^{2n}}(K_I g(A \gamma_+)). \quad (12b)$$

Notably, (12) corresponds to primal-dual dynamics of the augmented Lagrangian of (11). Thus, by [17, Theorem 4.5], the dynamics (12) are globally asymptotically stable with respect to a KKT point (γ_+^*, λ^*) of (11). In other words, (10) can be decomposed into dynamics that are globally asymptotically stable with respect to (γ_+^*, λ^*) and a constant γ_0 . Since $(\eta, \lambda) = (\Gamma_+ \gamma_+ + \Gamma_0 \gamma_0, \lambda) \in \mathcal{S}_\eta$ for any $\gamma_0 \in \mathbb{R}^{e \times e-(n-1)}$, it follows that (10) is globally asymptotically stable with respect to \mathcal{S}_η . The last statement of the Theorem follows by noting that $\frac{d}{dt}(\gamma_+, \lambda) = \mathbb{0}_{3n-1}$ when $(\gamma_+, \lambda) = (\gamma_+^*, \lambda^*)$ and $\frac{d}{dt} \gamma_0 = 0$. \square

The following corollary is a direct consequence of the proof of Theorem 3 and establishes that the optimizer of (8) is unique if the graph \mathcal{G} is a tree (i.e., corresponds to a radial power network).

Corollary 2 (Radial network) *Consider P_ℓ , P_u , P_L , and P^* such that Assumption 1 and Assumption 2 hold. If \mathcal{G} is a tree, then (10) is globally asymptotically stable with respect to the unique optimizer of (8), i.e., \mathcal{S}_η is a singleton.*

D. Power-limiting droop control in edge coordinates

To analyze power-limiting droop control in edge coordinates, let $C_\eta := [I_e \ \mathbb{0}_{e \times 2n}]$ and $T_\eta := \text{blkdiag}(VB^T, I_{2n})$.

Lemma 2 (Coinciding vector fields) *Let $\varphi_\theta(t, (\theta_0, \lambda_0))$ and $\varphi_\eta(t, (\eta_0, \lambda_0))$ denote the solutions of (3) and (10) for initial conditions (θ_0, λ_0) and (η_0, λ_0) . Then, it holds that*

- (i) $\eta(t) = C_\eta \varphi_\eta(t, (\eta_0, \lambda_0)) \in \text{Im}(VB^T)$ for all $t \in \mathbb{R}_{\geq 0}$ and all $\eta_0 \in \text{Im}(VB^T)$, and
- (ii) $T_\eta \varphi_\theta(t, (\theta_0, \lambda_0)) = \varphi_\eta(t, T_\eta(\theta_0, \lambda_0))$.

Proof. We first note that $\frac{d}{dt} \eta \in \text{Im}(VB^T)$ in (10). Therefore, for all $\eta_0 \in \text{Im}(VB^T)$, it holds that $C_\eta \varphi_\eta(t, (\eta_0, \lambda_0)) \in$

$\text{Im}(VB^T)$ for all $t \in \mathbb{R}_{\geq 0}$. To show statement (ii), let

$$\begin{aligned} f(\eta, \lambda) &:= M(P^* - P_L - BV\eta) - (\alpha \otimes K_I) \lambda \\ &\quad - (\alpha \otimes K_P) \Pi_{\mathbb{R}_{\geq 0}^n}(g(BV\eta)). \end{aligned}$$

Then (3) and (10) can be written as

$$VB^T \frac{d}{dt} \theta = VB^T f(\underbrace{VB^T \theta}_{=\eta}, \lambda) = \frac{d}{dt} \eta, \quad (13)$$

$$\frac{d}{dt} \lambda = \Pi_{\mathcal{T}_\lambda \mathbb{R}_{\geq 0}^{2n}} \left((I_2 \otimes K_I) g(BV \underbrace{VB^T \theta}_{=\eta}) \right). \quad (14)$$

In other words, the vector fields of (3) and (10) coincide mapped to the edge coordinates in the sense of statement (ii) (i.e., by multiplying (3) with T_η from the left) when $\eta \in \text{Im}(VB^T)$. \square

In other words, when starting from an initial condition such that $\eta_0 \in \text{Im}(VB^T)$, the dynamics (10) coincide with the dynamics (3) mapped to the edge coordinates.

E. Proof of the main results

We are now ready to prove our main results.

Proof of Theorem 1: First, we establish that there exist $\underline{\kappa} \in \mathbb{R}_{> 0}$ and $\bar{\kappa} \in \mathbb{R}_{\geq 0}$ such that

$$\underline{\kappa} \|T_\eta \varphi_\theta(t, \xi_0)\|_{\mathcal{S}_\eta} \leq \|\varphi_\theta(t, \xi_0)\|_{\mathcal{S}_\theta} \leq \bar{\kappa} \|T_\eta \varphi_\theta(t, \xi_0)\|_{\mathcal{S}_\eta} \quad (15)$$

holds for all $\xi_0 \in \mathbb{R}^n \times \mathbb{R}_{> 0}^{2n}$. To this end, we note that

$$\|T_\eta(\theta, \lambda)\|_{\mathcal{S}_\eta} = \min_{(\eta', \lambda') \in \mathcal{S}_\eta} \|(\eta' - VB^T \theta, \lambda' - \lambda)\|, \quad (16)$$

$$\|(\theta, \lambda)\|_{\mathcal{S}_\theta} = \min_{(\theta', \lambda') \in \mathcal{S}_\theta} \|(\theta' - \theta, \lambda' - \lambda)\| \quad (17)$$

and let $(\theta^*, \lambda^*) \in \mathcal{S}_\theta$ denote the (unique) optimizer of (17). Note that $(VB^T \theta^*, \lambda^*) \in \mathcal{S}_\eta$, by Cauchy–Schwarz inequality, it follows that

$$\|T_\eta(\theta^* - \theta, \lambda^* - \lambda)\| \leq \|T_\eta\| \|(\theta^* - \theta, \lambda^* - \lambda)\|,$$

i.e., any optimizer of (17) can be used to upper bound (16) in terms of (17). It immediately follows that the first inequality in (15) holds with $\underline{\kappa} = \|T_\eta\|^{-1} \in \mathbb{R}_{> 0}$. Next, let

$$\sigma_\perp := \min_{\theta \perp \mathbb{1}_n, \|\theta\|=1} \|VB^T \theta\| \in \mathbb{R}_{> 0},$$

and decompose $\eta' = VB^T \beta' + z' \in \mathbb{R}^e$ into $\beta' \in \mathbb{R}^n$ and $z' \perp \text{Im}(VB^T)$, i.e., $z' \in \ker(BV)$. Then, $\|T_\eta(\beta, \lambda)\|_{\mathcal{S}_\eta}$ can be written as

$$\begin{aligned} &\min_{(\beta', z', \lambda') : (VB^T \beta' + z', \lambda') \in \mathcal{S}_\eta} \|(VB^T(\beta' - \theta) + z', \lambda' - \lambda)\|, \\ &= \min_{(\beta', \lambda') : (VB^T \beta', \lambda') \in \mathcal{S}_\eta} \|(VB^T(\beta' - \theta), \lambda' - \lambda)\|, \end{aligned} \quad (18)$$

where we used that

$$\|VB^T y + z'\| = \sqrt{y^T L y + 2y^T B V z' + (z')^T z'},$$

with $y = \beta' - \theta$ and $BV z' = \mathbb{0}_n$ to conclude that the minimum of (18) is attained at $z' = \mathbb{0}_e$. In other words, for any (β', λ') such that $(VB^T \beta', \lambda') \in \mathcal{S}_\eta$ we obtain

$$\begin{aligned} \min_{\beta', \lambda'} \left\| \begin{bmatrix} VB^T(\beta' - \theta) \\ \lambda' - \lambda \end{bmatrix} \right\| &\geq \min_{\beta', \lambda'} \left\| \begin{bmatrix} \sigma_\perp I_n & \mathbb{0}_{n \times 2n} \\ \mathbb{0}_{2n \times n} & I_{2n} \end{bmatrix} \begin{bmatrix} \beta' - \theta \\ \lambda' - \lambda \end{bmatrix} \right\| \\ &\geq \min\{\sigma_\perp, 1\} \min_{\beta', \lambda'} \left\| \begin{bmatrix} \beta' - \theta \\ \lambda' - \lambda \end{bmatrix} \right\| \end{aligned}$$

and (15) holds with $\bar{\kappa} = \frac{1}{\min\{\sigma_{1,1}\}} \in \mathbb{R}_{>0}$. By Theorem 3, (10) is GAS on $\mathbb{R}^e \times \mathbb{R}_{>0}^{2n}$ with respect to \mathcal{S}_η . In other words, there exists $\chi_\eta \in \mathcal{X}\mathcal{L}$ such that

$$\|\varphi_\eta(t, T_\eta \xi_0)\|_{\mathcal{S}_\eta} \leq \chi_\eta(t, \|T_\eta \xi_0\|_{\mathcal{S}_\eta})$$

for all $\xi_0 \in \mathbb{R}^n \times \mathbb{R}_{>0}^{2n}$ and all $t \in \mathbb{R}_{\geq 0}$. Using Lemma 2, (15), and $\chi_\eta(t, \|T_\eta \xi_0\|_{\mathcal{S}_\eta}) \leq \chi_\eta(t, \underline{\kappa}^{-1} \|T_\eta \xi_0\|_{\mathcal{S}_\theta})$, we obtain

$$\|\varphi_\theta(t, \xi_0)\|_{\mathcal{S}_\theta} \leq \bar{\kappa} \|\varphi_\eta(t, T_\eta \xi_0)\|_{\mathcal{S}_\eta} \leq \bar{\kappa} \chi_\eta(t, \underline{\kappa}^{-1} \|T_\eta \xi_0\|_{\mathcal{S}_\theta})$$

for all $\xi_0 \in \mathbb{R}^n \times \mathbb{R}_{>0}^{2n}$ and all $t \in \mathbb{R}_{\geq 0}$. In other words, is globally asymptotically stable on $\mathbb{R}^n \times \mathbb{R}_{>0}^{2n}$ with respect to the set \mathcal{S}_θ . Finally, we show that $\lim_{t \rightarrow \infty} \omega(t) = \mathbb{1}_n \omega_s$. According to Theorem 3, any pair (η^*, λ^*) converges to a KKT point $(\eta^*, \lambda^*) \in \mathcal{S}_\eta$, i.e., $\lim_{t \rightarrow \infty} \eta(t) = \eta^*$ and $\lim_{t \rightarrow \infty} \frac{d}{dt} \eta = \mathbb{0}_e$. Using $\eta = VB^\top \theta$, we obtain

$$\lim_{t \rightarrow \infty} \frac{d}{dt} VB^\top \theta(t) = \lim_{t \rightarrow \infty} VB^\top \frac{d}{dt} \theta(t) = \lim_{t \rightarrow \infty} VB^\top \omega(t) = \mathbb{0}$$

and $\lim_{t \rightarrow \infty} \omega(t) = \mathbb{1}_n \omega_s$ follows $\ker(B^\top) = \text{span}(\mathbb{1}_n)$. \square

The next result formalizes that, upon convergence to \mathcal{S}_θ , if any converter is operating at the upper power limit, no converter can operate at the lower power limit and vice versa.

Proof of Proposition 2: We will proof the results by contradiction. For any KKT point $(\eta^*, \lambda^*) \in \mathcal{S}_\eta$, it holds that

$$M(BV\eta^* + P_L - P^*) + K_I(\lambda_{u,i}^* - \lambda_{\ell,i}^*) \in \ker(B^\top).$$

Moreover, $\ker(B^\top) = \text{span}(\mathbb{1}_n)$ and, by complementary slackness, $\lambda_{\ell,i}^* = 0$ and $\lambda_{u,j}^* = 0$ for any $(i, j) \in \mathcal{I}_u \times \mathcal{I}_\ell$. Thus,

$$m_i(P_i - P_i^*) + \sqrt{k_i} \lambda_{u,i}^* = m_j(P_j - P_j^*) - \sqrt{k_j} \lambda_{\ell,j}^*$$

has to hold for all $(i, j) \in \mathcal{I}_u \times \mathcal{I}_\ell$. By feasibility of $(\eta, \lambda^*) \in \mathcal{S}_\eta$ and, we have $P_i = P_{u,i}$ for all $i \in \mathcal{I}_u$ and $P_j = P_{\ell,j}$ for all $j \in \mathcal{I}_\ell$. Then, dual-feasibility and Assumption 2 imply that

$$m_i \underbrace{(P_{u,i} - P_i^*)}_{>0} + \underbrace{\sqrt{k_i} \lambda_{u,i}^*}_{\geq 0} = m_i \underbrace{(P_{\ell,i} - P_j^*)}_{<0} - \underbrace{\sqrt{k_j} \lambda_{\ell,j}^*}_{\geq 0},$$

i.e., no pair $(i, j) \in \mathcal{I}_u \times \mathcal{I}_\ell$ can exist if $(\eta^*, \lambda^*) \in \mathcal{S}_\eta$. \square

Proof of Theorem 2: By Theorem 1, there exists $(\theta^*, \lambda^*) \in \mathcal{S}_\theta$ such that

$$\lim_{t \rightarrow \infty} \omega(t) = M(P^* - P_L - L\theta^*) - (\alpha \otimes K_I)\lambda^* = \mathbb{1}_n \omega_s.$$

Where we have used (3a) and the fact that $\Pi_{\mathbb{R}_{\geq 0}^{2n}}(g(L\theta^*)) = \mathbb{0}_{2n}$ for all $(\theta^*, \lambda^*) \in \mathcal{S}_\theta$. Using $P = L\theta + P_L$ it follows that

$$m_i^{-1} \omega_s = P_i^* - P_i + m_i^{-1} \sqrt{k_i} (\lambda_{\ell,i}^* - \lambda_{u,i}^*), \quad \forall i \in \mathcal{N}. \quad (19)$$

Since $\lambda_{u,i}^* = \lambda_{\ell,i}^* = 0$ for all $i \notin \mathcal{I}_u \cup \mathcal{I}_\ell$, we obtain

$$\sum_{i \notin \mathcal{I}_u \cup \mathcal{I}_\ell} m_i^{-1} \omega_s = \sum_{i \notin \mathcal{I}_u \cup \mathcal{I}_\ell} P_i^* - \sum_{i \notin \mathcal{I}_u \cup \mathcal{I}_\ell} P_i. \quad (20)$$

Moreover, considering $\mathbb{1}_n^\top (L\theta + P_L) = \mathbb{1}_n^\top P_L$ it follows that $\sum_{i \in \mathcal{N}} P_i = \sum_{i \in \mathcal{N}} P_{L,i}$ and

$$\sum_{i \notin \mathcal{I}_u \cup \mathcal{I}_\ell} P_i + \sum_{i \in \mathcal{I}_\ell} P_{\ell,i} + \sum_{i \in \mathcal{I}_u} P_{u,i} = \sum_{i \in \mathcal{N}} P_{L,i}.$$

Solving for $\sum_{i \notin \mathcal{I}_u \cup \mathcal{I}_\ell} P_i$ and substituting into (20), results in

$$\sum_{i \notin \mathcal{I}_u \cup \mathcal{I}_\ell} m_i^{-1} \omega_s = \sum_{i \notin \mathcal{I}_u \cup \mathcal{I}_\ell} P_i^* + \sum_{i \in \mathcal{I}_u} P_{u,i} + \sum_{i \in \mathcal{I}_\ell} P_{\ell,i} - \sum_{i \in \mathcal{N}} P_{L,i}$$

and

$$\omega_s = \frac{\sum_{i \notin \mathcal{I}_u \cup \mathcal{I}_\ell} P_i^* + \sum_{i \in \mathcal{I}_u} P_{u,i} + \sum_{i \in \mathcal{I}_\ell} P_{\ell,i} - \sum_{i \in \mathcal{N}} P_{L,i}}{\sum_{i \notin \mathcal{I}_u \cup \mathcal{I}_\ell} m_i^{-1}}. \quad (21)$$

To show (i), consider $\mathcal{I}_\ell \neq \emptyset$. Then, by Proposition 2, $\mathcal{I}_u = \emptyset$. Moreover, (i) $\lambda_{\ell,i} \geq 0$ by dual feasibility, (ii) $\lambda_{u,i} = 0$ by complementary slackness, and (iii) $P_i^* - P_{\ell,i} > 0$ for all $\forall i \in \mathcal{N}$ by Assumption 2. Then (19) results in

$$\omega_s = \omega_i = m_i(P_i^* - P_{\ell,i}) + \sqrt{k_i}(\lambda_{\ell,i} - \lambda_{u,i}) > 0, \quad \forall i \in \mathcal{I}_\ell,$$

i.e., $\omega_s > 0$ holds. Moreover, (21) and $\mathcal{I}_u = \emptyset$ imply that

$$\sum_{i \notin \mathcal{I}_\ell} P_i^* + \sum_{i \in \mathcal{I}_\ell} P_{\ell,i} - \sum_{i \in \mathcal{N}} P_{L,i} > 0.$$

Additionally, Assumption 1 implies $\sum_{i \in \mathcal{I}_\ell} P_{\ell,i} < \sum_{i \in \mathcal{I}_\ell} P_i^*$, i.e.,

$$\sum_{i \in \mathcal{N}} P_i^* - \sum_{i \in \mathcal{N}} P_{L,i} > \sum_{i \notin \mathcal{I}_\ell} P_i^* + \sum_{i \in \mathcal{I}_\ell} P_{\ell,i} - \sum_{i \in \mathcal{N}} P_{L,i} > 0,$$

i.e., $\sum_{i \in \mathcal{N}} P_{L,i} < \sum_{i \in \mathcal{N}} P_i^*$. Assuming from $\mathcal{I}_u \neq \emptyset$ and applying the same steps used for showing (i) establishes (iii).

It remains to show (ii). To this end, assume that $\mathcal{I}_\ell = \emptyset$. Using $\sum_{i \in \mathcal{N}} P_{L,i} = \sum_{i \in \mathcal{N}} P_i^*$, the synchronous frequency reduces to

$$\omega_s = \frac{\sum_{i \in \mathcal{I}_u} P_{u,i} - P_i^*}{\sum_{i \notin \mathcal{I}_u} m_i^{-1}} > 0.$$

However, (i) $\lambda_{u,i} \geq 0$ by primal feasibility, (ii) $\lambda_{\ell,i} = 0$, by complementary slackness, and (iii) $P_i^* - P_{u,i} < 0$ for all $i \in \mathcal{N}$ by Assumption 2. This results in

$$\omega_s = \omega_i = m_i(P_i^* - P_{u,i}) - \sqrt{k_i} \lambda_{u,i} < 0, \quad \forall i \in \mathcal{I}_u,$$

and it follows that $\mathcal{I}_u = \mathcal{I}_\ell = \emptyset$. Following the same steps for $\mathcal{I}_u = \emptyset$ and $\sum_{i \in \mathcal{N}} P_{L,i} = \sum_{i \in \mathcal{N}} P_i^*$ shows that $\mathcal{I}_\ell = \emptyset$ has to hold. The Theorem follows by noting that either $\mathcal{I}_u = \emptyset$ or $\mathcal{I}_\ell = \emptyset$ by Proposition 2. \square

Proof of Corollary 1: Statement (i) and statement (ii) are direct consequences of Proposition 2 and the proof of Theorem 2. Statement (iii) can be shown by contradiction. In particular, $\sum_{i \in \mathcal{N}} P_{L,i} < \sum_{i \in \mathcal{N}} P_i^*$ implies $\omega_s > 0$. However, per the proof of Theorem 2, if there exists $i \in \mathcal{I}_u \neq \emptyset$, then $\omega_s < 0$. Thus, $\mathcal{I}_u = \emptyset$ has to hold. Statement (iv) follows by noting that $\sum_{i \in \mathcal{N}} P_{L,i} > \sum_{i \in \mathcal{N}} P_i^*$ implies $\omega_s < 0$. However, per the proof of Theorem 2, if there exists $i \in \mathcal{I}_\ell \neq \emptyset$, then $\omega_s > 0$. Thus, $\mathcal{I}_\ell = \emptyset$ has to hold. \square

V. CONCLUSIONS AND OUTLOOK

In this paper, we analytically studied the frequency dynamics of power systems comprised of power converters using power-limiting droop control. We provided a detailed stability analysis and characterized the synchronous frequency and power-sharing of power-limiting droop control. To this end, we represented the frequency dynamics of a network of converters using power-limiting droop control as a projected dynamical system. Next, we proposed a constrained power flow problem that aims to minimize the deviation of converter power injections from their dispatch under power limits. The

power system frequency dynamics and constrained power flow problem are formulated in coordinates associated with each converter (i.e., nodal coordinates). Notably, changing coordinates to edge coordinates associated with transmission lines, the frequency dynamics of a network of converters using power-limiting droop control in edge coordinates become identical to the primal-dual dynamics associated with the inequality constrained optimization problem.

Leveraging convergence results for primal-dual dynamics, we show that, under mild assumptions, the frequency dynamics of network of converters using power-limiting droop control are globally asymptotically stable with respect to set of KKT points of the underlying constrained power flow problem. Furthermore, we established that (i) the converters synchronize to a common synchronous frequency, and (ii) exhibit power-sharing properties similar to conventional unconstrained droop control. Specifically, we analyzed the impact of power limits on the synchronous steady-state frequency of the power system and characterized the synchronous frequency in terms of overall total load, sum of converter power setpoints, and converter droop coefficients. Particularly, converters share additional load according to their droop coefficients up to their power limit. Moreover, we established that power-limiting droop control does not converge to counter-intuitive operating points at which some converters operate at their upper limit while others are at their lower limit.

While these results are encouraging, future work should consider a wider range of constraints and voltage magnitude dynamics. In particular, converter current limits, converter dc voltage limits, and resource (e.g., renewable generation) constraints beyond active power limits (e.g., wind turbine speed limits) are seen as interesting topics for future work.

REFERENCES

- [1] B. Kroposki, B. Johnson, Y. Zhang, V. Gevorgian, P. Denholm, B.-M. Hodge, and B. Hannegan, "Achieving a 100% renewable grid: Operating electric power systems with extremely high levels of variable renewable energy," *IEEE Power and Energy Magazine*, vol. 15, no. 2, pp. 61–73, 2017.
- [2] F. Milano, F. Dörfler, G. Hug, D. J. Hill, and G. Verbič, "Foundations and challenges of low-inertia systems (invited paper)," in *Power Systems Computation Conference (PSCC)*, 2018.
- [3] B. Kroposki and A. Hoke, "A path to 100 percent renewable energy: Grid-forming inverters will give us the grid we need now," *IEEE Spectrum*, vol. 61, no. 5, pp. 50–57, 2024.
- [4] A. Tayyebi, D. Groß, A. Anta, F. Kupzog, and F. Dörfler, "Frequency stability of synchronous machines and grid-forming power converters," *IEEE Journal of Emerging and Selected Topics in Power Electronics*, vol. 8, no. 2, pp. 1004–1018, 2020.
- [5] M. Chandorkar, D. Divan, and R. Adapa, "Control of parallel connected inverters in stand-alone ac supply systems," *IEEE Trans. Ind. Appl.*, vol. 29, no. 1, pp. 136–143, 1993.
- [6] S. D'Árco, J. A. Suul, and O. B. Fosfo, "A virtual synchronous machine implementation for distributed control of power converters in smart-grids," *Electric Power Systems Research*, vol. 122, pp. 180–197, 2015.
- [7] D. Groß, M. Colombino, J.-S. Brouillon, and F. Dörfler, "The effect of transmission-line dynamics on grid-forming dispatchable virtual oscillator control," *IEEE Transactions on Control of Network Systems*, vol. 6, no. 3, pp. 1148–1160, 2019.
- [8] F. Dörfler and F. Bullo, "Synchronization and transient stability in power networks and nonuniform kuramoto oscillators," *SIAM Journal on Control and Optimization*, vol. 50, no. 3, pp. 1616–1642, 2012.
- [9] J. Schiffer, D. Goldin, J. Raisch, and T. Sezi, "Synchronization of droop-controlled microgrids with distributed rotational and electronic generation," in *IEEE Conf. on Dec. and Control*, 2013, pp. 2334–2339.
- [10] I. Subotić, D. Groß, M. Colombino, and F. Dörfler, "A Lyapunov framework for nested dynamical systems on multiple time scales with application to converter-based power systems," *IEEE Transactions on Automatic Control*, vol. 66, no. 12, pp. 5909–5924, 2021.
- [11] F. Salha, F. Colas, and X. Guillaud, "Virtual resistance principle for the overcurrent protection of pwm voltage source inverter," in *IEEE PES Innovative Smart Grid Technologies Conference Europe*, 2010.
- [12] A. D. Paquette and D. M. Divan, "Virtual impedance current limiting for inverters in microgrids with synchronous generators," *IEEE Transactions on Industry Applications*, vol. 51, no. 2, pp. 1630–1638, 2015.
- [13] B. Fan, T. Liu, F. Zhao, H. Wu, and X. Wang, "A review of current-limiting control of grid-forming inverters under symmetrical disturbances," *IEEE Open Journal of Power Electronics*, vol. 3, pp. 955–969, 2022.
- [14] N. Baeckeland, D. Chatterjee, M. Lu, B. Johnson, and G.-S. Seo, "Overcurrent limiting in grid-forming inverters: A comprehensive review and discussion," *IEEE Transactions on Power Electronics*, vol. 39, no. 11, pp. 14493–14517, 2024.
- [15] Z. Chen, D. Pattabiraman, R. H. Lasseter, and T. M. Jahns, "Certs microgrids with photovoltaic microsources and feeder flow control," in *IEEE Energy Conversion Congress and Exposition (ECCE)*, 2016.
- [16] W. Du, R. H. Lasseter, and A. S. Khalsa, "Survivability of autonomous microgrid during overload events," *IEEE Trans. Smart Grid*, vol. 10, no. 4, pp. 3515–3524, 2019.
- [17] A. Cherukuri, E. Mallada, and J. Cortés, "Asymptotic convergence of constrained primal-dual dynamics," *Systems & Control Letters*, vol. 87, pp. 10–15, 2016.
- [18] N. Li, C. Zhao, and L. Chen, "Connecting automatic generation control and economic dispatch from an optimization view," *IEEE Transactions on Control of Network Systems*, vol. 3, no. 3, pp. 254–264, 2016.
- [19] M. Colombino, E. Dall'Anese, and A. Bernstein, "Online optimization as a feedback controller: Stability and tracking," *IEEE Transactions on Control of Network Systems*, vol. 7, no. 1, pp. 422–432, 2020.
- [20] G. Qu and N. Li, "On the exponential stability of primal-dual gradient dynamics," *IEEE Control Systems Letters*, vol. 3, no. 1, pp. 43–48, 2019.
- [21] D. Zelazo and M. Mesbahi, "Edge agreement: Graph-theoretic performance bounds and passivity analysis," *IEEE Trans. Autom. Control*, vol. 56, no. 3, pp. 544–555, 2011.
- [22] J. W. Simpson-Porco, F. Dörfler, and F. Bullo, "Synchronization and power sharing for droop-controlled inverters in islanded microgrids," *Automatica*, vol. 49, no. 9, pp. 2603–2611, 2013.
- [23] F. Dörfler and F. Bullo, "Kron reduction of graphs with applications to electrical networks," *IEEE Trans. Circuits Syst. I*, vol. 60, no. 1, pp. 150–163, 2013.
- [24] F. Bullo, *Lectures on Network Systems*, 1.7 ed., 2024.
- [25] P. Piagi and R. Lasseter, "Autonomous control of microgrids," in *IEEE Power Engineering Society General Meeting (PESGM)*, 2006.
- [26] J. Rocabert, A. Luna, F. Blaabjerg, and P. Rodríguez, "Control of power converters in ac microgrids," *IEEE Trans. Power Electron.*, vol. 27, no. 11, pp. 4734–4749, 2012.
- [27] J. Schiffer, R. Ortega, A. Astolfi, J. Raisch, and T. Sezi, "Conditions for stability of droop-controlled inverter-based microgrids," *Automatica*, vol. 50, no. 10, pp. 2457–2469, 2014.
- [28] P. Dupuis and A. Nagurney, "Dynamical systems and variational inequalities," *Annals of Operations Research*, vol. 44, no. 1, pp. 7–42, 1993.
- [29] A. Hauswirth, S. Bolognani, and F. Dörfler, "Projected dynamical systems on irregular, non-euclidean domains for nonlinear optimization," *SIAM Journal on Control and Optimization*, vol. 59, no. 1, pp. 635–668, 2021.
- [30] C. L. Jean-Baptiste Hiriart-Urruty, *Convex Analysis and Minimization Algorithms I*. Springer Berlin, Heidelberg, 1993.
- [31] S. Boyd and L. Vandenberghe, *Convex Optimization*. Cambridge University Press, 2004.
- [32] D. Angeli, "An almost global notion of input-to-state stability," *IEEE Transactions on Automatic Control*, vol. 49, no. 6, pp. 866–874, 2004.
- [33] W. Hahn, *Stability of Motion*, ser. Grundlehren der mathematischen Wissenschaften. Springer Berlin Heidelberg, 1967.
- [34] C. M. Kellett, "A compendium of comparison function results," *Mathematics of Control, Signals, and Systems*, vol. 26, no. 3, pp. 339–374, 2014.
- [35] D. Zelazo and M. Bürger, "On the definiteness of the weighted laplacian and its connection to effective resistance," in *IEEE Conf. on Dec. and Control*, 2014, pp. 2895–2900.
- [36] R. Horn and C. Johnson, *Matrix Analysis*, 2nd ed. Cambridge University Press, 2013.